ACS APPLIED MATERIALS & INTERFACES

Research Article

www.acsami.org

(TFPP)Eu[Pc(OPh)$_8$]Eu[Pc(OPh)$_8$]/CuPc Two-Component Bilayer Heterojunction-Based Organic Transistors with High Ambipolar Performance

Dameng Gao,[†] Xia Zhang,[†] Xia Kong,[†] Yanli Chen,*[,†] and Jianzhuang Jiang*[,‡]

[†]Shandong Provincial Key Laboratory of Fluorine Chemistry and Chemical Materials, School of Chemistry and Chemical Engineering, University of Jinan, Jinan 250022, China

[‡]Beijing Key Laboratory for Science and Application of Functional Molecular and Crystalline Materials, Department of Chemistry, University of Science and Technology Beijing, Beijing 100083, China

Supporting Information

ABSTRACT: Organic thin film transistor (OTFT) devices fabricated by the solution-based QLS technique from a mixed (phthalocyaninato)-(porphyrinato) europium complex (TFPP)Eu[Pc(OPh)$_8$]Eu[Pc(OPh)$_8$] exhibit air-stable ambipolar performance with mobilities of 6.0×10^{-5} cm^2 V^{-1} s^{-}1 for holes and 1.4×10^{-4} cm^2 V^{-1} s^{-1} for electrons, respectively. In good contrast, the two-component bilayer heterojunction thin film devices constructed by directly growing (TFPP)Eu[Pc(OPh)$_8$]Eu[Pc-(OPh)$_8$] on vacuum deposited (VCD) CuPc film using solution based QLS method were revealed to show unprecedented ambipolar performance with carrier mobilities of 0.16 cm^2 V^{-1} s^{-1} for holes and 0.30 cm^2 V^{-1} s^{-1} for electrons. In addition to the intrinsic role of p-type organic semiconductor, the VCD CuPc film on the substrate also acts as a good template that induces significant improvement over the molecular ordering of triple-decker compound in the film. In particular, it results in the change in the aggregation mode of (TFPP)Eu[Pc(OPh)$_8$]Eu[Pc(OPh)$_8$] from J-type in the single-layer film to H-type in the bilayer film according to the UV−vis, XRD, and AFM observations.

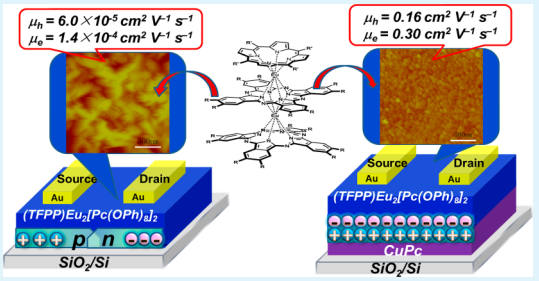

KEYWORDS: *phthalocyanine, triple-decker, ambipolar, OTFT, organic heterojunction*

INTRODUCTION

Great progress has been made in organic thin film transistors (OTFTs) since the first reports on p-type OTFTs based on in 1980s.[1−3] For the purpose of constructing organic integrated electronic circuits with a wide range of potential industrial applications,[4−6] the thin film transistors exhibiting ambipolar behavior that are able to simultaneously provide both n- and p-channel performance in single device also become highly desired in addition to the unipolar (either holes or electrons) behaved OTFTs.[7−10] Since the fabrication of the first OTFT with both p and n channels from the bis(phthalocyaninato) lutetium double-decker compound in 1990 (despite the lack of term "ambipolar" by the authors at that time),[11] different methods have been developed thus far for fabricating ambipolar OTFTs, which can be classified in terms of the composition of semiconducting layer, including the single-component thin film, two-component bilayer thin film, and two-component blending thin film-based ambipolar OTFTs.[7−10] Significant progress has been achieved over the ambipolar OTFTs that are based on single-component with suitable HOMO and LUMO energy levels which ensure the simultaneous stable electron and hole transport as well as the efficient injection of both charge carriers from the same metal electrode in particular in recent years.[7,8,12,13] This, however, seems not true for either the two-component bilayer or the blending two-component ambipolar OTFTs because of the much more difficulty toward understanding their working mechanism associated with the involvement of more than one component despite the great efforts paid in this direction.[9,10,14−21] In 1995, in order to achieve the ambipolar device performance, Dodabalapur and co-workers tried to combine the p-type α-hexathienylene and n-type C_{60} semiconductors together by means of the bilayer technique, affording the first two-component active layers OTFTs with relative balanced carrier mobilities of 4×10^{-3} cm^2 V^{-1} s^{-1} for holes and 5×10^{-3} cm^2 V^{-1} s^{-1} for electrons, respectively, under vacuum.[14] This certainly aroused significant research interests, initiating a relatively wide range of investigations over the two-component bilayer thin film transistors with different combination of p-type and n-type organic semiconductors including polymers and in particular small molecules like pentacene/C_{60},[15] CuPc/F_{16}CuPc,[16] BP_2T/F_{16}CuPc,[17] pentacenue/PTCDI-$C_{13}H_{27}$,[18] and DH4T/PTCDI-$C_{13}H_{27}$.[19] To the best of our knowledge, the best result was achieved for the pentacene/C_{60} p−n heterostructure bilayer

Received: October 23, 2014
Accepted: January 20, 2015
Published: January 20, 2015

DOI: 10.1021/am507353s
ACS Appl. Mater. Interfaces 2015, 7, 2486−2493

OTFTs with the electron and hole mobilities reaching the order of 0.1 $cm^2\ V^{-1}\ s^{-1}$.[12] Interestingly, the p−p isotype bilayer heterojunction OTFTs consisting of both the wide band gap *p*-type unipolar 2,2′;7′,2″-terphenanthrenyl (Ph3) and the narrow band gap p-type unipolar vanadyl-phthalocyanine (VOPc) were revealed to present the best ambipolar OTFTs performance with the air-stable balanced carrier mobilities up to 0.45 and 0.28 $cm^2\ V^{-1}\ s^{-1}$ for holes and electrons, respectively, despite the still not clear completely reason at this stage.[20] As part of our continuous effort toward the fabrication of high-performance phthalocyanine-based organic field effect transistors in particular the amipolar OTFTs,[13,22−24] in the present case, we describe the fabrication of novel two-component bilayer thin film transistors based on the intrinsic ambipolar organic semiconductor of sandwich mixed (phthalocyaninato)(porphyrinato) europium triple-decker (TFPP)Eu[Pc(OPh)$_8$]Eu[Pc(OPh)$_8$] [TFPP = dianion of 5,10,15,20-tetrakis(*p*-fluorophenyl)porphyrin; Pc(OPh)$_8$ = dianion of 2,3,9,10,16,17,23,24-octa(phenoxy)phthalocyanine], Scheme 1, in combination with the p-type unipolar organic semiconductor of CuPc with good and balanced ambipolar transporting properties in air.

Scheme 1. Schematic Molecular Structure of the Sandwich Mixed (Phthalocyaninato)(Porphyrinato) Europium (TFPP)Eu[Pc(OPh)$_8$]Eu[Pc(OPh)$_8$] (1)

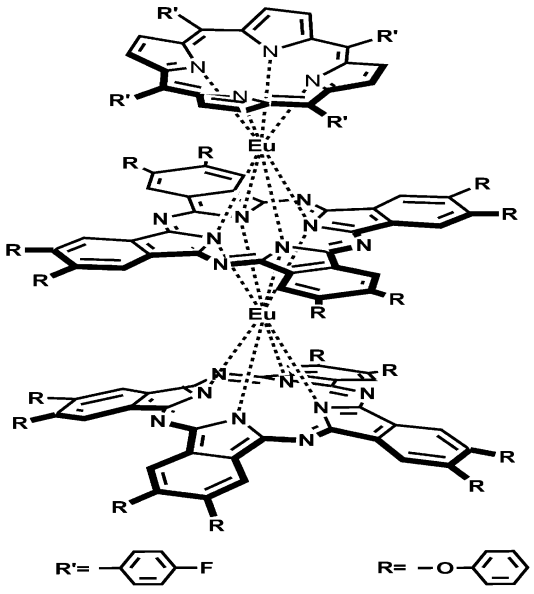

EXPERIMENTAL SECTION

General. The mixed (phthalocyaninato)(porphyrinato) europium complex (TFPP)Eu[Pc(OPh)$_8$]Eu[Pc(OPh)$_8$] (**1**) was prepared following the published procedures.[25−28] Phthalocyaninato copper (CuPc) was purchased from Aldrich and used as received. Electrochemical measurement was carried out with a CHI760D voltammetric analyzer. The cell comprised inlets for a glassy carbon disk working electrode of 3.0 mm in diameter and a silver-wire counter electrode. The reference electrode was Ag/Ag^+ (0.01 mol dm^{-3}), which was connected to the solution by a Luggin capillary, whose tip was placed close to the working electrode. It was corrected for junction potentials by being referenced internally to the ferrocenium/ferrocene (Fc^+/Fc) couple [$E_{1/2}$(Fc^+/Fc) = 0.50 V vs SCE]. Typically, a 0.1 mol dm^{-3} solution of [Bu_4N][ClO_4] in CH_2Cl_2 containing 0.5 mmol dm^{-3} of sample was purged with nitrogen for 5 min, then the voltammogram was recorded at ambient temperature. Electronic absorption spectra were recorded on a Hitachi U-4100 spectrophotometer. X-ray diffraction experiment was carried out on a Bruker D8 FOCUS X-ray diffractometer. AFM images were collected under ambient conditions using the tapping mode with a NanoscopeIII/Bioscope scanning probe microscope from Digital instruments.

Fabrication of the Thin Films. Thin films deposition was conducted as following: (i) CuPc VCD film: CuPc film was deposited on substrates (quartz and SiO_2/Si) by means of classical thermal evaporation (using a ZZS 660 system) from a tantalum boat at ca. 1×10^{-6} mbar and a 2 Å s^{-1} rate. The deposition rate and film thickness were monitored by quartz crystal microbalance. This layer is typically 30 to 50 nm thick. (ii) Quasi-Langmuir−Shäfer (QLS) film: 5.0 mL of chloroform solution of (TFPP)Eu[Pc(OPh)$_8$]Eu[Pc(OPh)$_8$] (**1**) ($\sim 1 \times 10^{-6}$ mol L^{-1}) was put into a cylindrical glass container (diameter, 9.5 cm; height, 1.5 cm; volume, 106.3 cm^3), then 65 mL of water was slowly added onto the container (***caution**: the amount of water added cannot completely cover the surface of the chloroform solution so as to maintain a path for the evaporation of the solvent, $CHCl_3$*). During the solvent evaporation, the triple-decker molecules gradually assembled to form some fine nanostructures at the $CHCl_3$/water interface and in turn the densely packed film on the water surface until complete evaporation of $CHCl_3$. The film can be easily transferred from the water surface onto a quartz or SiO_2/Si substrate by horizontal lifting, i.e., the slide was horizontally and carefully lowered onto the film surface and then raised.[29] This process was repeated to obtain the required number of layers. Residual water on the substrate, between transfer steps and after the final transfer, was removed with a stream of N_2. (iii) (TFPP)Eu[Pc(OPh)$_8$]Eu[Pc(OPh)$_8$]/CuPc heterojunction film: Some fine nanostructures of (TFPP)Eu[Pc(OPh)$_8$]Eu[Pc(OPh)$_8$] formed at the $CHCl_3$/water interface were transferred via repeating the deposition (QLS film) onto the CuPc VCD film, resulting in a (TFPP)Eu[Pc(OPh)$_8$]Eu[Pc(OPh)$_8$]/CuPc bilayer heterojunction. In the present case, the 20-layer (TFPP)Eu[Pc(OPh)$_8$]Eu[Pc(OPh)$_8$] QLS film is obtained as either the single-component film or the second-layer in (TFPP)Eu[Pc(OPh)$_8$]Eu[Pc(OPh)$_8$]/CuPc bilayer heterojunction. The deposition process mentioned above is similar to those reported previously for the preparation of resistors[29] and MSDIs (semiconductor-doped insulator heterojunctions).[30]

Fabrication and Measurements of OTFT Devices. OTFT devices were fabricated on a SiO_2/Si (300 nm thickness, capacitance C_0 = 10 nF cm^{-2}) substrate by evaporating gold electrodes onto both the (TFPP)Eu[Pc(OPh)$_8$]Eu[Pc(OPh)$_8$] QLS films and the bilayer films employing a shadow mask. These electrodes have a width (W) of 28.6 mm and a channel length (L) of 0.24 mm. The ratio of the width to length (W/L) of the channel was then 119. The drain-source current (I_{ds}) versus drain-source voltage (V_{ds}) characteristic was obtained with a Hewlett-Packard (HP) 4140B parameter analyzer at room temperature. It is noteworthy that no additional surface treatment was carried out on the bare SiO_2/Si substrate except the cleaning procedure by means of the sonication in chloroform, acetone, and ultrahigh-purity water in order to remove the possible organic contamination.

RESULTS AND DISCUSSION

Molecular Design, Synthesis, and Electrochemistry. Previous investigations have revealed the potential ambipolar organic semiconducting nature, also with potential balanced carrier mobilities between electrons and holes, of sandwich-type heteroleptic tris(tetrapyrrole) rare earth triple-decker complexes containing different tetrapyrrole ligands with suitable HOMO and LUMO energy levels relative to the working functional of gold electrodes.[24] As a consequence, in the present case mixed (phthalocyaninato)(porphyrinato) europium triple-decker complex (TFPP)Eu[Pc(OPh)$_8$]Eu[Pc(OPh)$_8$] (**1**) was prepared according to published procedure and characterized by a series of spectroscopic methods including MALDI-TOF mass and ^{1}H NMR, Figure S1 and

DOI: 10.1021/am507353s
ACS Appl. Mater. Interfaces 2015, 7, 2486−2493

S2 (Supporting Information). Four *p*-fluorophenyl substituents with slight electron-withdrawing ability[13] were introduced onto the meso-positions of porphyrin ligand, whereas eight phenoxyl moieties also with very weak electron-withdrawing ability[31,32] were introduced onto the peripheral positions of the phthalocyanine ligands, in the mixed (phthalocyaninato)-(porphyrinato) europium triple-decker molecule to tune its HOMO and in particular the LUMO energy level toward enhancing the hole and in particular electron transport of corresponding organic semiconductor.[13] Cyclic voltammetrical (CV) measurement over this triple-decker compound in CH_2Cl_2 disclosed four reversible one-electron redox couples with the first oxidation and first reduction potential at +0.64 and −0.54 V (vs SCE), Figure 1 and Table S1 (Supporting Information). The HOMO and LUMO energies locating at −5.08 and −3.90 eV, respectively, thus derived for this triple-decker just simultaneously meet the energy range required for good p-type and n-type organic semiconductors,[33,34] suggesting the ambipolar organic semiconducting nature of this triple-decker complex.

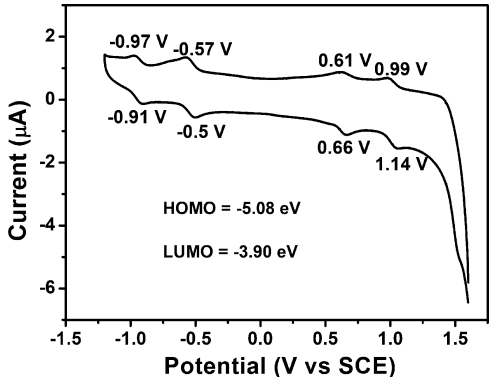

Figure 1. Cyclic voltammogram (CV) of (TFPP)Eu[Pc(OPh)$_8$]Eu-[Pc(OPh)$_8$] in CH_2Cl_2 containing 0.1 mol L^{-1} [Bu_4N][ClO_4] at a scan rate of 20 mV s^{-1}.

OTFTs Characterization. As clearly exhibited in Figure 2A, the OTFTs device fabricated from **1** on the SiO_2/Si substrate using the QLS technique with a bottom-gate top-contact configuration showed typically ambipolar (both p-channel and n-channel) characteristics under ambient conditions, indicating the air-stable intrinsic ambipolar semiconducting nature of this compound. The carrier mobility (μ) can be calculated by using the saturation region transistor equation, $I_{ds} = (W/2L)\mu C_0(V_G - V_T)^2$, where I_{ds} is the source-drain current, V_G the gate voltage, C_0 the capacitance per unit area of the dielectric layer, and V_T the threshold voltage,[35] resulting in the carrier mobilities for holes of 6.0×10^{-5} cm^2 V^{-1} s^{-1} and for electrons of 1.4×10^{-4} cm^2 V^{-1} s^{-1}, Figure 2A. Very interestingly, after being fabricated into the two-component bilayer heterojunction thin film field effect transistors together with the p-type unipolar semiconductor CuPc by directly growing of (TFPP)-Eu[Pc(OPh)$_8$]Eu[Pc(OPh)$_8$] on the vacuum deposited (VCD) CuPc film using the solution-based QLS method, the devices constructed also exhibited air-stable performance with typical ambipolar nature, but with significant improvement over the carrier mobilities for both holes and electrons, up to 0.16 and 0.30 cm^2 V^{-1} s^{-1}, respectively, Figure 2B and Table S2 (Supporting Information). It should be pointed out that totally 30 efficient devices were examined. From the saturation-regime

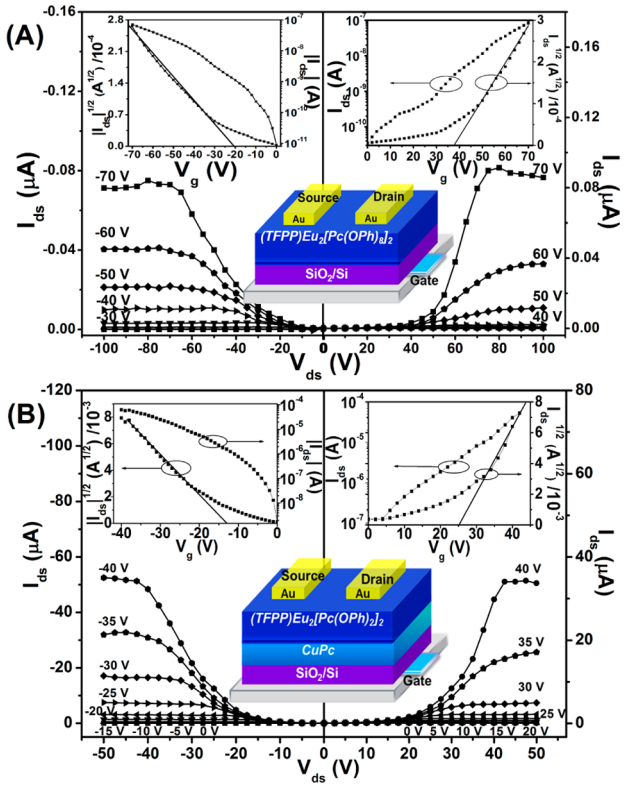

Figure 2. Output characteristics (I_{ds} versus V_{ds}) and (insets) transfer characteristics ($|I_{ds}|^{1/2}$ versus V_g) as well as device configurations of ambipolar OTFTs based on (A) the single-component (TFPP)Eu-[Pc(OPh)$_8$]Eu[Pc(OPh)$_8$] QLS film and (B) two-component (TFPP)Eu[Pc(OPh)$_8$]Eu[Pc(OPh)$_8$]/CuPc heterojunction deposited on SiO_2/Si (300 nm) substrate with Au top contact measured in air.

transfer plots, we estimated the hole mobility of 0.16 ± 0.01 cm^2 V^{-1} s^{-1} and electron mobility of 0.30 ± 0.01 cm^2 V^{-1} s^{-1}. The distribution of devices mobility is shown in Figure S3 (Supporting Information). After having been stored in air for 2 months, the OTFTs exhibit negligible change in both electron and hole mobilities, Figure S4 and Table S2 (Supporting Information), indicating the good stability of the devices in air. To the best of our knowledge, these results are actually among the best ambipolar performance in terms of the scale of carrier mobilities for both holes and electrons and in particular the balance between them for the two-component bilayer OTFT devices under ambient conditions.[10,36] For comparative purposes, the transport performance of the single layer CuPc VCD film-based OTFTs grown under the same condition as that in the bilayer heterojunction has also been recorded. As displayed in Figure S5 and Table S2 (Supporting Information), these single-layer CuPc VCD film-based OTFTs exhibited relative low hole mobility of 0.0014 cm^2 V^{-1} s^{-1} in comparison with the bilayer heterojunction devices. This is consistent with the results reported previously.[37] It is also worth noting that the threshold voltages (V_T) were decreased from the single-component-based device (−20 V for hole and +38 V for electron) to the two-component-based device (−13 V for hole and +25 V for electron), indicating the decrease in the trap states in the bilayer heterojunction film.[2,3,11,20,21] In addition, as evidenced by the nonlinearity of the output curve at low source-drain voltage, both the single- and two-component-based devices show significant contact resistance due to the presence of charge carrier trap states within the solution-based

DOI: 10.1021/am507353s
ACS Appl. Mater. Interfaces 2015, 7, 2486−2493

film and at the semiconductor-metal interface.[16] However, electron and hole injection from gold into the (TFPP)Eu[Pc(OPh)$_8$]Eu[Pc(OPh)$_8$]/CuPc two-component bilayer heterojunction is still efficient because of the heterojunction effect: the electrons and holes accumulated at the interface of bilayer heterojunction fill the trap states under the applied gate field in the two-component device.[38] Furthermore, both the output and transfer curves for either single-component (TFPP)Eu[Pc(OPh)$_8$]Eu[Pc(OPh)$_8$] OTFTs or two-component bilayer ambipolar devices in the present case at low gate voltages do not show the current increase in a superlinear manner at high source-drain voltages, ensuring their future practical applications. This is in line with those observed for ambipolar OFET devices reported previously.[14,39−42]

Thin Films Microstructures and Morphologies. For the purpose of clarifying the large carrier mobilities of the two-component heterojunction devices relative to the single-component QLS film, analysis over the molecular packing mode of (TFPP)Eu[Pc(OPh)$_8$]Eu[Pc(OPh)$_8$] triple-decker molecules in the films and the internal film-structure has been conducted on the basis of the UV−vis absorption spectra, thin-film XRD, and AFM observations. As shown in Figure 3,

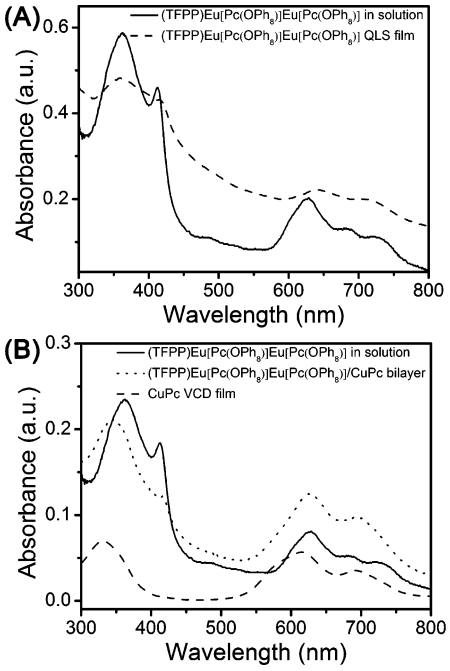

Figure 3. UV−vis absorption spectra of (TFPP)Eu[Pc(OPh)$_8$]Eu[Pc(OPh)$_8$] in $CHCl_3$ solution (solid line) and (A) QLS film (dashed line); (B) CuPc film (dashed line) and the (TFPP)Eu[Pc(OPh)$_8$]Eu[Pc(OPh)$_8$]/CuPc bilayer (dotted line).

(TFPP)Eu[Pc(OPh)$_8$]Eu[Pc(OPh)$_8$] in $CHCl_3$ solution displays intense Soret bands at 362 and 412 nm and the main Q-bands at 629 nm with two weak vibrational shoulders at 687 and 720 nm, in line with those reports for mixed (phthalocyaninato)(porphyrinato) rare earth triple-decker analogues.[24,43] However, after being fabricated into the QLS film, the two main Q-bands were broadened and red-shifted to 641 and 714 nm, respectively, while the Soret band at 412 nm was red-shifted to 415 nm, Figure 3A, indicating the formation of *J*-type (edge-to-edge) molecular packing structure in the QLS films of **1**, on the basis of exciton theory[44] and previously published results.[23] As for the CuPc VCD film, Figure 3B, the absorption due to the $\pi-\pi^*$ transitions of phthalocyanine macrocycle appeared in the visible region at 615 and 694 nm (Q-bands), showing as a doublet due to Davydov splitting.[30] The intensity of the higher energy peak at 615 nm is larger than that for the lower energy peak at 694 nm, indicating a typical α-CuPc phase.[45] In addition, the Q-band of the CuPc VCD film is broadened and blue-shifted with respect to CuPc in solution,[46] revealing the formation of a H-type (face-to-face) molecular packing structure and strong intermolecular interactions between phthalocyanine rings. These results are in good accordance with those deduced from the XRD studies as detailed below. As shown in Figure 3B, the UV−vis spectrum of the (TFPP)Eu[Pc(OPh)$_8$]Eu[Pc(OPh)$_8$]/CuPc bilayer heterojunction film showed two distinct Q-bands at 625 and 694 nm. Obviously, the latter well-defined lower energy peak at 694 nm should be mainly contributed from the α-CuPc film, suggesting the same molecular packing mode of CuPc molecules in both the single layer film and the bilayer heterojunction film. This is further confirmed by thin-film XRD result (vide infra). Although the former broadened Q-band at 625 nm is attributed to the combination of the blue-shifted Q absorption of (TFPP)Eu[Pc(OPh)$_8$]Eu[Pc(OPh)$_8$] and the higher energy peak of the CuPc film. This seems also true for the Soret bands of (TFPP)Eu[Pc(OPh)$_8$]Eu[Pc(OPh)$_8$] in the bilayer heterojunction film, Figure 3B. On the basis of Kasha's exciton theory, blue-shifts in the main absorption bands of (TFPP)Eu[Pc(OPh)$_8$]Eu[Pc(OPh)$_8$] in the bilayer heterojunction film are a typically sign of the effective face-to-face $\pi-\pi$ interaction between tetrapyrrole ligands of neighboring triple-decker molecules, indicating the successful change in the aggregation mode of (TFPP)Eu[Pc(OPh)$_8$]Eu[Pc(OPh)$_8$] molecules from *J*-type in the single-component QLS film to H-type in the bilayer heterojunction film and in particular the important role of the VCD CuPc film in inducing the change of (TFPP)Eu[Pc(OPh)$_8$]Eu[Pc(OPh)$_8$] molecular packing mode. Obviously, the much more effective intermolecular face-to-face interaction in the H-aggregates of triple-decker molecules than that in the J-aggregates provides the electrons (as well as holes) with a more extensive area for delocalization, which in turn is responsible for the much larger carrier mobilities revealed for the devices fabricated from the bilayer heterojunction film than the single-component QLS film.[42,47]

The quality of the single film and bilayer heterojunction film as well as the preferred molecular orientation has been assessed using the out-of-plane (OOP) X-ray diffraction (XRD) technique. As shown in Figure 4A, the OOP XRD diagram of the CuPc VCD film shows only one sharp diffraction peak at $2\theta = 6.86°$ ($d = 1.29$ nm) because of the interstacking distance of the α-phase (200) lattice planes, indicating the nearly perpendicular orientation of the CuPc molecules to the substrate surface in a face-to-face stack within the thin film.[48] In the OOP XRD pattern of the single-component QLS film of (TFPP)Eu[Pc(OPh)$_8$]Eu[Pc(OPh)$_8$], Figure 4B, two well-defined peaks originating from the (100) and (010) plane are observed at 2.05 and 3.57 nm, respectively. These two diffraction peaks should be assigned to the dimensional size for a unit cell, 2.05 nm (thickness) × 3.57 nm (length), formed from edge-to-edge (J-type) stacking of two triple-decker molecules depending on the $\pi-\pi$ stacking and the van der Waals intermolecular interactions between neighboring triple-decker molecules on the basis of the energy-optimized molecular structure according to our previous studies.[13,23,24] The XRD pattern of (TFPP)Eu[Pc(OPh)$_8$]Eu[Pc(OPh)$_8$]/

DOI: 10.1021/am507353s
ACS Appl. Mater. Interfaces 2015, 7, 2486−2493

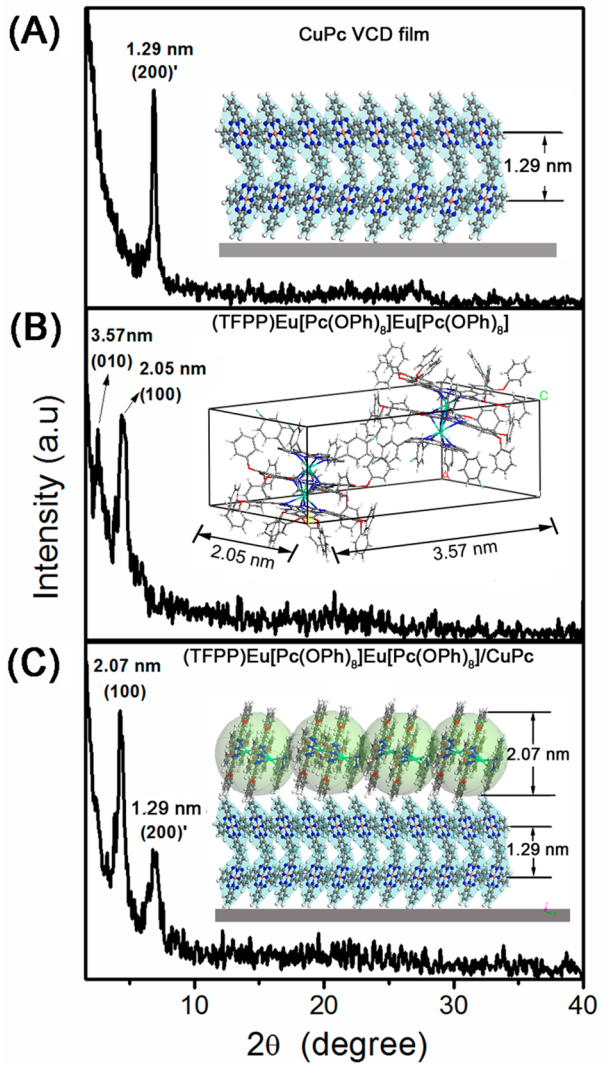

Figure 4. X-ray patterns for the (A) CuPc, (B) (TFPP)Eu[Pc(OPh)$_8$]Eu[Pc(OPh)$_8$], and (C) (TFPP)Eu[Pc(OPh)$_8$]Eu[Pc(OPh)$_8$]/CuPc thin films deposited on SiO_2/Si substrates.

CuPc bilayer heterojunction film displays two peaks at 2θ = 4.27° (d = 2.07 nm) and 6.88° (d = 1.29 nm), corresponding to the (100) lattice plane of the top-layer (TFPP)Eu[Pc(OPh)$_8$]Eu[Pc(OPh)$_8$] and (200) lattice plane of the sublayer (CuPc), respectively,[45,49] Figure 4C. Appearance of the peak resulting from the diffraction of the α-CuPc (200) lattice plane in the bilayer heterojunction film indicates the same molecular stacking structure employed by the CuPc molecules in the bilayer heterojunction film as in the single-component CuPc VCD film. In addition, observation of the d-spacing of 2.07 nm due to the thickness of one (TFPP)Eu[Pc(OPh)$_8$]Eu[Pc(OPh)$_8$] layer also in the bilayer heterojunction film suggests the regular layered structure of the triple-decker QLS film in the heterojunction.[29,50,51] Judging from the diagonal dimension of the (TFPP)Eu[Pc(OPh)$_8$]Eu[Pc(OPh)$_8$] molecule, 2.20 nm, on the basis of single crystal X-ray diffraction results,[26,31] the orientation angle between the phthalocyanine plane in the triple-decker molecule and substrate surface should amount to ca.70.2°. This indicates the "edge-on" conformation of the triple-decker molecules in the bilayer heterojunction film. As a consequence, the triple-decker molecules employ nearly a perpendicular orientation to the substrate surface in a H-aggregation mode in the QLS layer of the bilayer heterojunction film,[52] inset of Figure 4C. This is in good contrast to the J-aggregation mode employed by triple-decker molecules in the single-component QLS film as detailed above, indicating again the template role of the α-CuPc (200) lattice plane in inducing the change of the aggregation mode for the triple-decker molecules from J-type in single-component QLS film to H-type in the two-component bilayer heterojunction film in addition to acting as the intrinsic active layer. The cofacial molecular stacking mode with the "edge-on" configuration for both CuPc and (TFPP)Eu[Pc(OPh)$_8$]Eu[Pc(OPh)$_8$] molecules in the bilayer heterojunction film, is favorable for the carrier transportation at the interface of the two phases.[23,53] This is responsible for the significant improvement over the device performance in particular for the ambipolar charge transport in a bilayer organic thin-film transistors.

AFM observations are able to provide more information on the aspect of the films and therefore allow the correlation between the morphology and electrical properties. Figure 5 compares the morphology of the (TFPP)Eu[Pc(OPh)$_8$]Eu[Pc(OPh)$_8$] QLS film deposited on the SiO_2/Si substrate with that deposited on the CuPc VCD film as substrate. For the comparison purpose, the CuPc VCD film morphology has also been displayed in Figure 5B. As can be seen in Figure 5A, the (TFPP)Eu[Pc(OPh)$_8$]Eu[Pc(OPh)$_8$] QLS film deposited directly on the SiO_2/Si substrate forms a randomly distributed sheet-like aggregates of ca. 500 nm in length with large gaps and cracks between aggregate domains and a root-mean-square (R_{rms}) value as high as 30.7 nm. This definitely does not favor

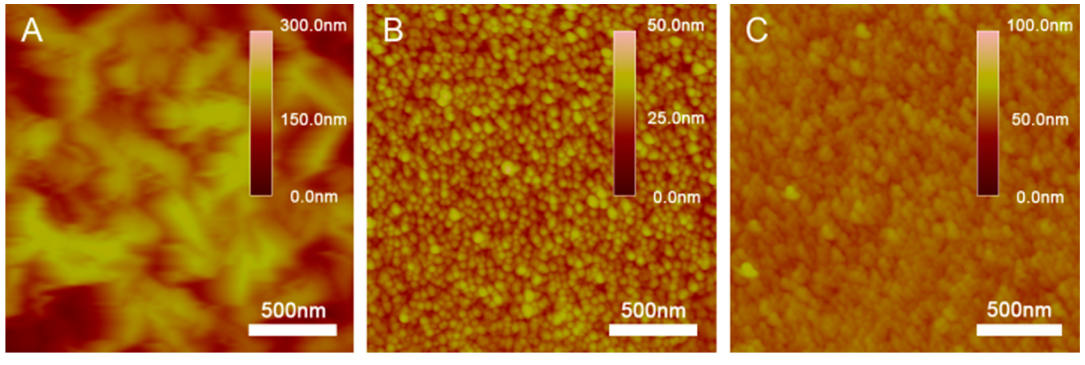

Figure 5. AFM images of (A) (TFPP)Eu[Pc(OPh)$_8$]Eu[Pc(OPh)$_8$] QLS film grown on the bare SiO_2/Si substrate, (B) CuPc VCD film grown on the bare SiO_2/Si substrate, and (C) (TFPP)Eu[Pc(OPh)$_8$]Eu[Pc(OPh)$_8$] QLS film grown on CuPc film substrate.

DOI: 10.1021/am507353s
ACS Appl. Mater. Interfaces 2015, 7, 2486−2493

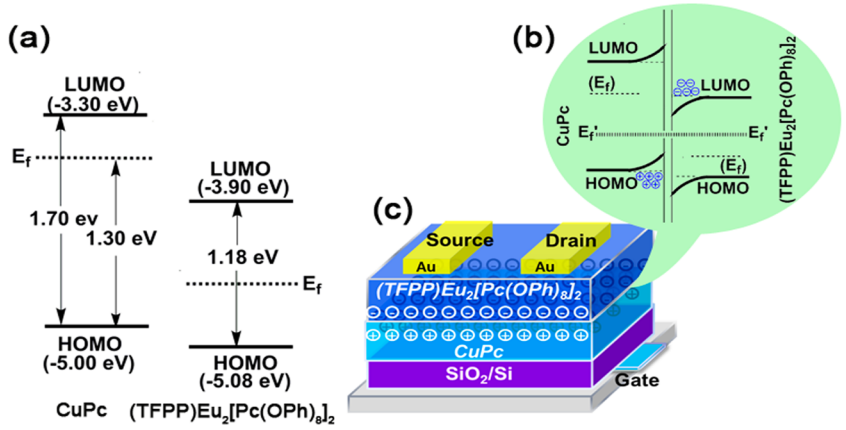

Figure 6. Schematic energy levels of CuPc and (TFPP)Eu[Pc(OPh)$_8$]Eu[Pc(OPh)$_8$] (a) before and (b) after contact together with the (c) scheme of the heterojunction effect in the heterojunction transistor, with mobile free electrons and holes shown in the accumulated region of charge carriers of the heterojunction. E_f and E_f' represent Fermi levels before and after contact, respectively.

the charge transport in this film and therefore is responsible for the relatively lower carrier mobilities for both holes and electrons of the single-component film OTFTs. The CuPc VCD film consists of uniform small grain crystallites with approximately 70 nm in diameter, giving a R_{rms} roughness value of 6.84 nm, Figure 5B. Meanwhile, some voids are also observed in the CuPc film that provides locations upon which the second triple-decker molecular layer is able to grow. As expected, significant improvement over the morphology has been achieved over the QLS film after being fabricated onto the CuPc VCD film as substrate, Figure 5C. Many crystallites of ca. 100 nm in diameter with good connection between crystallites grains and the R_{rms} value as small as 3.31 nm have been clearly revealed for the (TFPP)Eu[Pc(OPh)$_8$]Eu[Pc(OPh)$_8$] film deposited on the CuPc-modified substrate. This is surely beneficial for the charge transport and therefore results in significant improvement over the OTFT device performance.

Transistor Mechanism. Despite the difference in the composition from the previously reported two-component bilayer thin film devices in terms of the organic semiconductors nature, the remarkably improved device performance of the heterojunction devices relative to the single-component QLS film-based OTFTs in the present case should also be due to the heterojunction effect (accumulation of electrons and holes occurs in the interface of bilayer heterojunction).[38] The energy levels of both CuPc and (TFPP)Eu[Pc(OPh)$_8$]Eu[Pc(OPh)$_8$] (**1**) are shown in Figure 6a, based on the electrochemical study of **1** and previously reported results for CuPc.[54] As can be found, (TFPP)Eu[Pc(OPh)$_8$]Eu[Pc(OPh)$_8$] accepts electrons more easily than CuPc due to its lower LUMO energy relative to the latter one, −3.90 versus −3.30 eV. As a result, the work function (the energy required to remove an electron from the semiconductor to the vacuum level), which is the difference between the vacuum level and the Fermi level (E_f), is lower for the (TFPP)Eu[Pc(OPh)$_8$]Eu[Pc(OPh)$_8$] layer than that for the CuPc layer, 3.7 eV.[54] When the two semiconductors contact each other to form a bilayer heterojunction, electrons spontaneously transfer from the CuPc layer to the (TFPP)Eu[Pc(OPh)$_8$]Eu[Pc(OPh)$_8$] one in the interface, while holes migrate into the CuPc layer. At the equilibrium state, the Fermi levels are aligned, leading to electron-accumulation in the (TFPP)Eu[Pc(OPh)$_8$]Eu[Pc(OPh)$_8$] layer side and hole-accumulation in the CuPc layer side, Figure 6b and 6c. This in turn results in an increase in the carrier mobility in the heterojunction transistors due to the abundance of mobile free carriers (electrons and holes). Meanwhile, the decrease in the threshold voltages for both holes and electrons can also be attributed to the accumulated electrons and holes in the interface of bilayer heterojunction (the heterojunction effect), which filled the trap states.[20,21]

CONCLUSION

A new mixed (phthalocyaninato)(porphyrinato)europium triple-decker compound with intrinsic air-stable ambipolar semiconducting nature has been designed, synthesized, and fabricated into the two-component bilayer heterojunction thin film OTFTs in combination with the *p*-type single-polar semiconductor CuPc for the first time. The resulting OTFT device has good performance with carrier mobilities of 0.16 cm^2 V^{-1} s^{-1} for holes and 0.30 cm^2 V^{-1} s^{-1} for electrons in air. This device surpasses many other competitors in terms of both scale and balance between the hole and electron mobility. The present work opens a new way for the preparation of air-stable, high-performance ambipolar OTFT devices through the combination of molecular design and device fabrication technique.

ASSOCIATED CONTENT

Supporting Information

Synthesis and characterization details of (TFPP)Eu[Pc(OPh)$_8$]Eu[Pc(OPh)$_8$] and ^{1}H NMR, MS, electrochemical, and OTFT data. This material is available free of charge via the Internet at http://pubs.acs.org.

AUTHOR INFORMATION

Corresponding Authors

*E-mail: chm_chenyl@ujn.edu.cn.
*E-mail: jianzhuang@ustb.edu.cn.

Notes

The authors declare no competing financial interest.

ACKNOWLEDGMENTS

This work was financially supported by the National Key Basic Research Program of China (2013CB933402 and 2012CB224801) and the National Natural Science Foundation of China (21290174 and 21371073).

DOI: 10.1021/am507353s
ACS Appl. Mater. Interfaces 2015, 7, 2486−2493

REFERENCES

(1) Tsumura, A.; Koezuka, H.; Ando, T. Macromolecular Electronic Device: Field-Effect Transistor with a Polythiophene Thin Film. *Appl. Phys. Lett.* **1986**, *49*, 1210−1212.

(2) Madru, M.; Guillaud, G.; Sadoun, M. A.; Maitrot, M.; Clarisse, C.; Contellec, M. L.; André, J. J.; Simon, J. The First Field Effect Transistor Based on an Intrinsic Molecular Semiconductor. *Chem. Phys. Lett.* **1987**, *142*, 103−105.

(3) Madru, R.; Guillaud, G.; Sadoun, M. A.; Maitrot, M.; André, J. J.; Simon, J.; Even, R. A Well-Behaved Field Effect Transistor Based on an Intrinsic Molecular Semiconductor. *Chem. Phys. Lett.* **1988**, *145*, 343−346.

(4) Usta, H.; Risko, C.; Wang, Z.; Huang, H.; Deliomeroglu, M.; Zhukhovitskiy, A.; Facchetti, A.; Marks, T. Design, Synthesis, and Characterization of Ladder-Type Molecules and Polymers. Air-Stable, Solution-Processable n-Channel and Ambipolar Semiconductors for Thin-Film Transistors via Experiment and Theory. *J. Am. Chem. Soc.* **2009**, *131*, 5586−5608.

(5) Guo, Y.; Yu, G.; Liu, Y. Organic FETs: Functional Organic Field-Effect Transistors. *Adv. Mater.* **2010**, *22*, 4427−4447.

(6) Sonar, P.; Singh, S.; Li, Y.; Soh, M.; Dodabalapur, A. A Low-Bandgap Diketopyrrolopyrrole-Benzothiadiazole-Based Copolymer for High-Mobility Ambipolar Organic Thin-Film Transistors. *Adv. Mater.* **2010**, *22*, 5409−5413.

(7) Wu, W.; Liu, Y.; Zhu, D. π-Conjugated Molecules with Fused Rings for Organic Field-Effect Transistors: Design, Synthesis and Applications. *Chem. Soc. Rev.* **2010**, *39*, 1489−1502.

(8) Ortiz, R. P.; Facchetti, A.; Marks, T. J. High-k Organic, Inorganic, and Hybrid Dielectrics for Low-Voltage Organic Field-Effect Transistors. *Chem. Rev.* **2010**, *110*, 205−239.

(9) Zaumseil, J.; Sirringhaus, H. Electron and Ambipolar Transport in Organic Field-Effect Transistors. *Chem. Rev.* **2007**, *107*, 1296−1323.

(10) Bisri, S. Z.; Piliego, C.; Gao, J.; Loi, M. A. Outlook and Emerging Semiconducting Materials for Ambipolar Transistors. *Adv. Mater.* **2014**, *26*, 1176−1199.

(11) Guillaud, G.; Sadoun, M. A.; Maitrot, M.; Simon, J.; Bouvet, M. Field-Effect Transistors Based on Intrinsic Molecular Semiconductors. *Chem. Phys. Lett.* **1990**, *167*, 503−506.

(12) Liang, Z.; Tang, Q.; Mao, R.; Liu, D.; Xu, J.; Miao, Q. The Position of Nitrogen in N-Heteropentacenes Matters. *Adv. Mater.* **2011**, *23*, 5514−5518.

(13) Kan, J.; Chen, Y.; Qi, D.; Liu, Y.; Jiang, J. High-Performance Air-Stable Ambipolar Organic Field-Effect Transistor Based on Tris-(phthalocyaninato) Europium(III). *Adv. Mater.* **2012**, *24*, 1755−1758.

(14) Dodabalapur, A.; Katz, H.; Torsi, L.; Haddon, R. Organic Heterostructure Field-Èffect Transistors. *Science* **1995**, *269*, 1560−1562.

(15) Wang, S. D.; Kanai, K.; Ouchi, Y.; Seki, K. Bottom Contact Ambipolar Organic Thin Film Transistor and Organic Inverter Based On C_{60}/Pentacene Heterostructure. *Org. Electron.* **2006**, *7*, 457−464.

(16) Wang, J.; Wang, H.; Yan, X.; Huang, H.; Yan, D. Air-Stable Ambipolar Organic Field-Effect Transistors Based On Phthalocyanince Composites Heterojunction. *Chem. Phys. Lett.* **2005**, *407*, 87−90.

(17) Shi, J. W.; Wang, H. B.; Song, D.; Tian, H. K.; Geng, Y. H.; Yan, D. H. n-Channel, Ambipolar, and p-Channel Organic Heterojunction Transistors Fabricated with Various Film Morphologies. *Adv. Funct. Mater.* **2007**, *17*, 397−400.

(18) Unni, K. N. N.; Pandey, A. K.; Alem, S.; Nunzi, J. M. Ambipolar Organic Field-Effect Transistor Fabricated by Co-evaporation of Pentacene and N,N-ditridecylperylene-3,4,9,10-tetracarboxylic Diimide. *Chem. Phys. Lett.* **2006**, *421*, 554−557.

(19) Dinelli, F.; Capelli, R.; Loi, M. A.; Murgia, M.; Muccini, M.; Facchetti, A.; Marks, T. J. High-Mobility Ambipolar Transport in Organic Light-Emitting Transistors. *Adv. Mater.* **2006**, *18*, 1416−1420.

(20) Wang, H.; Wang, X.; Yu, B.; Geng, Y.; Yan, D. Isotype Organic Heterojunction and Ambipolar Field-Effect Transistors. *Appl. Phys. Lett.* **2008**, *93*, 113303.

(21) Wang, H.; Yan, D. Organic Heterostructures in Organic Field-Effect Transistors. *Asia Mater.* **2010**, *2*, 69−78.

(22) Chen, Y.; Su, W.; Bai, M.; Jiang, J.; Li, X.; Liu, Y.; Wang, L.; Wang, S. High Performance Organic Field-Effect Transistors Based on Amphiphilic Tris(phthalocyaninato) Rare Earth Triple-Decker Complexes. *J. Am. Chem. Soc.* **2005**, *127*, 15700−15701.

(23) Li, D.; Wang, H.; Kan, J.; Lu, W.; Chen, Y.; Jiang, J. H-aggregation Mode in Triple-Decker Phthalocyaninato-Europium Semiconductors. Materials Design for High-Performance Air-Stable Ambipolar Organic Thin Film Transistors. *Org. Electron.* **2013**, *14*, 2582−2589.

(24) Zhang, X.; Chen, Y. A Sandwich Mixed (Phthalocyaninato) (Porphyrinato) Europium Triple-Decker: Balanced-Mobility, Ambipolar Organic Thin-Film Transistor. *Inorg. Chem. Commun.* **2014**, *39*, 79−82.

(25) Adler, A. D.; Longo, F. R.; Finarelli, J. D.; Goldmacher, J.; Assour, J.; Korsakoff, L. A Simplified Synthesis for Meso-tetraphenylporphine. *J. Org. Chem.* **1967**, *32*, 476.

(26) Lapkina, L.; Niskanen, E.; Rönkkömäki, H.; Larchenko, V.; Popov, K.; Tsivadze, A. Synthesis and Characterization of Sandwich-type Gadolinium and Ytterbium Crown Ether-Substituted Phthalocyanines. *J. Porphyrins Phthalocyanines* **2000**, *4*, 588−590.

(27) Jiang, J.; Liu, W.; Arnold, D. Sandwich Complexes of Naphthalocyanine with The Rare Earth Metals. *J. Porphyrins Phthalocyanines* **2003**, *7*, 459−473.

(28) Zhang, Y.; Jiang, W.; Jiang, J.; Xue, Q. Synthesis and Liquid Crystal Behavior of Tris[2,3,9,10,16,17,23,24-Octakis(Octyloxy)-Phthalocyaninato] Rare Earth Complexes. *J. Porphyrins Phthalocyanines* **2007**, *11*, 100−108.

(29) Chen, Y.; Bouvet, M.; Sizun, T.; Gao, Y.; Plassard, C.; Lesniewska, E.; Jiang, J. Facile Approaches to Build Ordered Amphiphilic Tris (Phthalocyaninato) Europium Triple-Decker Complex Thin Films and Their Comparative Performances in Ozone Sensing. *Phys. Chem. Chem. Phys.* **2010**, *12*, 12851−12861.

(30) Chen, Y.; Bouvet, M.; Sizun, T.; Barochi, G.; Rossignol, J.; Lesniewska, E. Enhanced Chemosensing of Ammonia Based on The Novel Molecular Semiconductor-Doped Insulator (MSDI) Heterojunctions. *Sens. Actuators, B* **2011**, *155*, 165−173.

(31) Lu, G.; Bai, M.; Li, R.; Zhang, X.; Ma, C.; Lo, P.-C.; Ng, D. K. P.; Jiang, J. Lanthanide(III) Double-Decker Complexes with Octaphenoxy- or Octathiophenoxyphthalocyaninato Ligands − Revealing the Electron-Withdrawing Nature of The Phenoxy and Thiophenoxy Groups in the Double-Decker Complexes. *Eur. J. Inorg. Chem.* **2006**, *18*, 3703−3709.

(32) Li, R.; Zhang, X.; Zhu, P.; Ng, D. K. P.; Kobayashi, N.; Jiang, J. Electron-Donating or-Withdrawing Nature of Substituents Revealed by The Electrochemistry of Metal-Free Phthalocyanines. *Inorg. Chem.* **2006**, *45*, 2327−2334.

(33) Tang, M. L.; Reichardt, A. D.; Wei, P.; Bao, Z. Correlating Carrier Type with Frontier Molecular Orbital Energy Levels in Organic Thin Film Transistors of Functionalized Acene Derivatives. *J. Am. Chem. Soc.* **2009**, *131*, 5264−5273.

(34) Zhao, Y.; Guo, Y.; Liu, Y. Anniversary Article: Recent Advances in n-Type and Ambipolar Organic Field-Effect Transistors. *Adv. Mater.* **2013**, *25*, 5372−5391.

(35) Sze, S. M.; Ng, K. K. *Physics of Semiconductor Devices*, 2nd ed.; Wiley: New York, 1981.

(36) Zhou, K.; Dong, H.; Zhang, H.; Hu, W. High Performance n-type and Ambipolar Small Organic Semiconductors for Organic Thin Film Transistors. *Phys. Chem. Chem. Phys.* **2014**, *16*, 22448−22457.

(37) Bao, Z.; Lovinger, A. J.; Dodabalapur, A. Organic Field-Effect Transistors with High Mobility Based on Copper Phthalocyanine. *Appl. Phys. Lett.* **1996**, *69*, 3066−3068.

(38) Wang, J.; Wang, H.; Yan, X.; Huang, H.; Jin, D.; Shi, J.; Tang, Y.; Yan, D. Heterojunction Ambipolar Organic Transistors Fabricated by a Two-Step Vacuum-Deposition Process. *Adv. Funct. Mater.* **2006**, *16*, 824−830.

(39) Song, C. L.; Ma, C. B.; Yang, F.; Zeng, W. J.; Zhang, H. L.; Gong, X. Synthesis of Tetrachloro-Azapentacene as an Ambipolar Organic Semiconductor with High and Balanced Carrier Mobilities. *Org. lett.* **2011**, *13*, 2880−2883.

DOI: 10.1021/am507353s
ACS Appl. Mater. Interfaces 2015, 7, 2486−2493

(40) Yamamoto, T.; Yasuda, T.; Sakai, Y.; Aramaki, S. Ambipolar Field-Effect Transistor (FET) and Redox Characteristics of a π-Conjugated Thiophene/1, 3, 4-Thiadiazole CT-Type Copolymer. *Macromol. Rapid Commun.* **2005**, *26*, 1214−1217.
(41) Liu, C.; Liu, Z.; Lemke, H. T.; Tsao, H. N.; Naber, R. C. G.; Li, Y.; Banger, K.; Müllen, K.; Nielsen, M. M.; Sirringhaus, H. High-Performance Solution-Deposited Ambipolar Organic Transistors Based on Terrylene Diimides. *Chem. Mater.* **2010**, *22*, 2120−2124.
(42) Locklin, J.; Shinbo, K.; Onishi, K.; Kaneko, F.; Bao, Z.; Advincula, R. C. Ambipolar Organic Thin Film Transistor-Like Behavior of Cationic and Anionic Phthalocyanines Fabricated Using Layer-by-Layer Deposition from Aqueous Solution. *Chem. Mater.* **2003**, *15*, 1404−1412.
(43) Lu, G.; Chen, Y.; Zhang, Y.; Bao, M.; Bian, Y.; Li, X.; Jiang, J. Morphology Controlled Self-Assembled Nanostructures of Sandwich Mixed (Phthalocyaninato)(Porphyrinato) Europium Triple-Deckers. Effect of Hydrogen Bonding on Tuning The Intermolecular Interaction. *J. Am. Chem. Soc.* **2008**, *130*, 11623−11630.
(44) Kasha, M.; Rawls, H. R.; EI-Bayoumi, M. A. The Exciton Model in Molecular Spectroscopy. *Pure Appl. Chem.* **1965**, *11*, 371−392.
(45) Padma, N.; Joshi, A.; Singh, A.; Deshpande, S. K.; Aswal, D. K.; Gupta, S. K.; Yakhmi, J. V. NO_2 Sensors with Room Temperature Operation and Long Term Stability Using Copper Phthalocyanine Thin Films. *Sens. Actuators, B* **2009**, *143*, 246−252.
(46) Chen, W. H.; Ko, W. Y.; Chen, Y. S.; Cheng, C. Y.; Chan, C. M.; Lin, K. J. Growth of Copper Phthalocyanine Rods on Au Plasmon Electrodes through Micelle Disruption Methods. *Langmuir* **2010**, *26*, 2191−2195.
(47) Anthony, J. E.; Brooks, J. S.; Eaton, D. L.; Parkin, S. R. Functionalized Pentacene: Improved Electronic Properties From Control of Solid-State Order. *J. Am. Chem. Soc.* **2001**, *123*, 9482−9483.
(48) Xiao, K.; Liu, Y.; Yu, G.; Zhu, D. Influence of The Substrate Temperature During Deposition on Film Characteristics of Copper Phthalocyanine and Field-Effect Transistor Properties. *Appl. Phys. A: Mater. Sci. Process.* **2003**, *77*, 367−370.
(49) Guillaud, G.; Simon, J. Transient Properties of Nickel Phthalocyanine Thin Film Transistors. *Chem. Phys. Lett.* **1994**, *219*, 123−126.
(50) Chen, Y.; Liu, H. G.; Pan, N.; Jiang, J. Langmuir−Blodgett Films of Substituted Bis (Naphthalocyaninato) Rare Earth Complexes: Structure and Interaction with Nitrogen Dioxide. *Thin Solid Films* **2004**, *460*, 279−285.
(51) Chen, Y.; Zhang, Y.; Zhu, P.; Fan, Y.; Bian, Y.; Li, X.; Jiang, J. Arrangement of Tris (Phthalocyaninato) Gadolinium Triple-Decker Complexes with Multi-Octyloxy Groups on Water Surface. *J. Colloid Interface Sci.* **2006**, *303*, 256−263.
(52) Meijer, E. J.; Leeuw, D. M. d.; Setayesh, S.; Veenendaal, E. V.; Huisman, B. H.; Blom, P. W. M.; Hummelen, J. C.; Scherf, U.; Klapwijk, T. M. Solution-Processed Ambipolar Organic Field-Effect Transistors and Inverters. *Nat. Mater.* **2003**, *2*, 678−682.
(53) Kim, S.; An, T. K.; Chen, J.; Kang, I.; Kang, S. H.; Chung, D. S.; Park, C. E.; Kim, Y. H.; Kwon, S. K. H-Aggregation Strategy in the Design of Molecular Semiconductors for Highly Reliable Organic Thin Film Transistors. *Adv. Funct. Mater.* **2011**, *21*, 1616−1623.
(54) Hill, I. G.; Kahn, A. Energy Level Alignment at Interfaces of Organic Semiconductor Heterostructures. *J. Appl. Phys.* **1998**, *84*, 5583−5586.

DOI: 10.1021/am507353s
ACS Appl. Mater. Interfaces 2015, 7, 2486−2493